Hyperthermic Ablation of Hepatic Tumors by Inductive Heating of Ferromagnetic Alloy Implants

Julie Androlowicz, Iain Clark, George Doerre, Nathan Netravali, Joseph Wynne

BEE 453: Computer Aided Design

May 5, 2003

Executive Summary

This study is an investigation into the ability of ferromagnetic thermal therapy to destroy cancerous hepatic tissue. Ferromagnetic rods are implanted in cancerous tissue and heated by induction. Increased temperatures result in tumor destruction. Because alloy implants are minimally invasive, used for multiple treatments and are temperature self-regulating, they represent a superior cancer treatment compared to many alternatives. The focus of modeling ferromagnetic thermal therapy will be to maximize tumor obliteration by considering heating temperature and the placement of alloy rods. Data on the efficacy of different Curie points and probe arrangements as well as sensitivity to variations in material properties are presented. Recommendations are made for the implementation of this treatment based on the modeled results.

Introduction and Design Objectives

In the mid nineteenth century a notable observation linked high body temperature caused by a fever to the regression of cancerous tissue. Subsequent studies have supported the relationship between temperature increase and tumor reduction (Tucker 2001). At temperatures of 45 C and above cellular proteins denature and membranes are destroyed (Tungjitkusolmun 2002). Thermal therapy has become a common and effective means of treatment of malignancies, although surgical resection is usually preferred. Of the thermal therapy treatment options, external beam radiation has had general success in tissue destruction (Tucker 2000). However, the inaccuracy of radiation can result in unwanted healthy tissue heating. Temperature monitoring is usually conducted to protect healthy tissue, requiring invasive probing of surrounding tissue (Paulus 1996). Another thermal therapy uses needle like electrodes to directly target tumors. Probe tips generate ionic vibrations producing enough frictional heat to ablate cancerous material. Although this method reduces the need for invasive monitoring, repeated treatment requires repeated probe insertion (Tungjitkusolmun 2002).

A relatively new treatment method eliminates many of the complications discussed above. Metal alloy rods can be inserted in cancerous tissue and heated inductively (Tucker 2000). When a patient with an implanted magnetic rod is placed within an alternating radio-frequency magnetic field, current flows through the implant and heat is generated (Tucker 2000). Heat production in the implant is predominately caused by eddy current loss. Consequently, only tissue surrounding the rod is heated (Paulus 1996).

The power output of a rod within a magnetic field is proportional its length, diameter, magnetic characteristics and the angle at which it lies with respect to the field. A ferromagnetic phenomenon called the Curie point makes inductive heating a temperature-regulated process (Paulus 1996). Upon reaching a set temperature the rod transitions from magnetic to paramagnetic and no heating beyond the set temperature can occur (Paulus 1996). By changing the percent of constituent elements in an alloy, the Curie point may be changed to suit a treatment type (Paulus 1997). Not only is the ferromagnetic rod self-regulating, but multiple treatments require no further invasive measures after the initial implant surgery. The only concern when using alloy implants is biocompatibility and the possibility of harmful decomposition. Based on a corrosion study comparing NiCu and PdCo, the Palladian Cobalt showed low decomposition in vitro and may be left implanted for long term cancer treatment (Paulus 1997). Ferromagnetic therapy of prostate cancer is in the clinical trial stages with encouraging success. With over a million new cases of liver carcinomas arising annually, initial research into the application of hepatic implants is warranted (Tungjitkusolmun 2002).

Computer-aided engineering will be used to model ferromagnetic tumor therapy in hepatic tissue. Simulating heating of an in-operable tumor will be conducted on a simple model. The model will consist of a cylindrical tumor with five metal alloy implants surrounded by healthy tissue. The objective is to destroy all cancerous material with little to no effect on the surrounding healthy tissue. With this in mind, determining the most effective Curie point and rod placement will be the focus of our project.

A schematic is provided below (Figure 1) to show how we modeled a tumor within the liver. The tumor is represented as a small cylindrical volume located within a spherical section of the liver. Additionally, Figure 2 shows a schematic of the placement of the probes. Each of the probes has a 0.5mm radius and a length of 14mm.

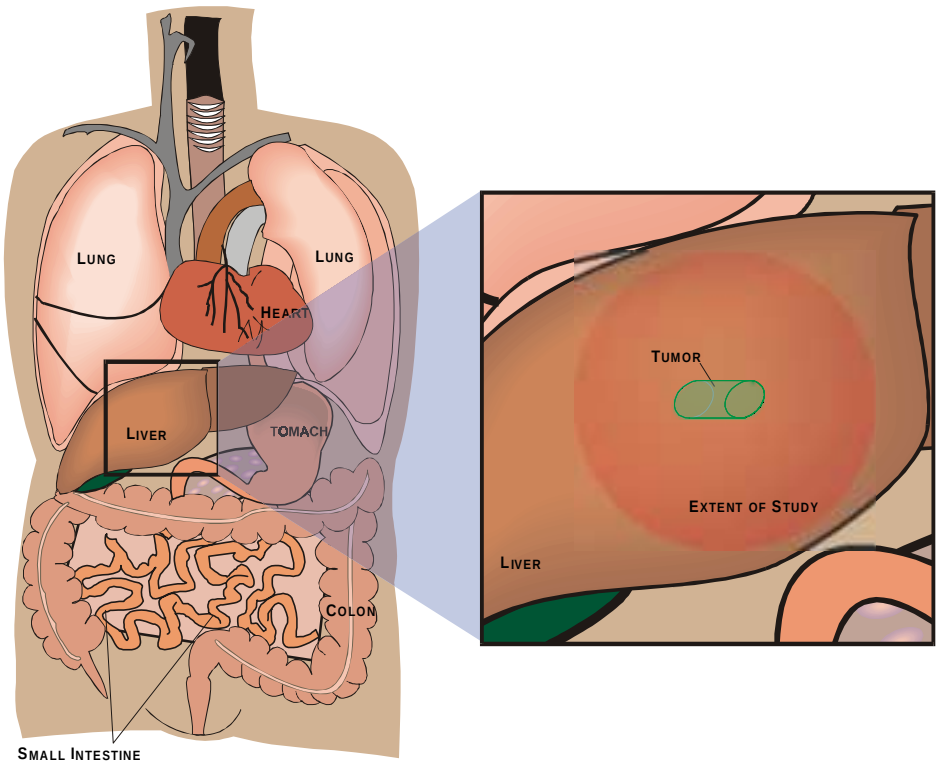

Figure 1: *The liver on the right ventral side of the midsection, below the lung. The tissue of the liver is generally homogeneous, especially within the dimensions of our areas of study. The close up view shows the relationship between a tumor and the adjacent area we are studying for adverse effects of the thermal ablation.*

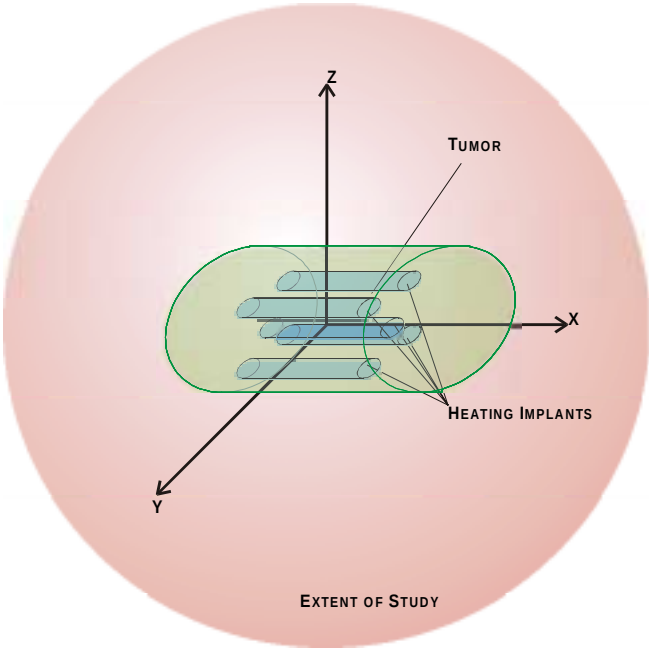

Figure 2: *A schematic of the geometry that we used for our simulation. The five-rod pattern gives good coverage in a centralized area. Four rods did not present sufficient heating in the central region of the tumor, except when energized to the point where an unacceptable amount of heat was transferred to surrounding tissue. The spacing of the rods was an important variable in our study.*

Results and Discussion

Curie Temperature

As discussed above, the Curie temperature is the temperature at which a ferromagnetic rod transitions from magnetic to paramagnetic. Rods may be manufactured to have a desired regulatory temperature. Figures 3 and 4 below show the effect of two different Curie temperatures on the temperature contour plot. The 70°C plot has the same shape as the 55°C plot. However on the 70°C plot, heating has propagated into the surrounding tissue to a greater degree. As expected, at the same time (600 seconds) the 70°C rods have heated a larger region to a greater temperature than the 55°C rods. (Note that colors on the 70°C plot correspond to different temperatures than the colors on the 55°C plot.)

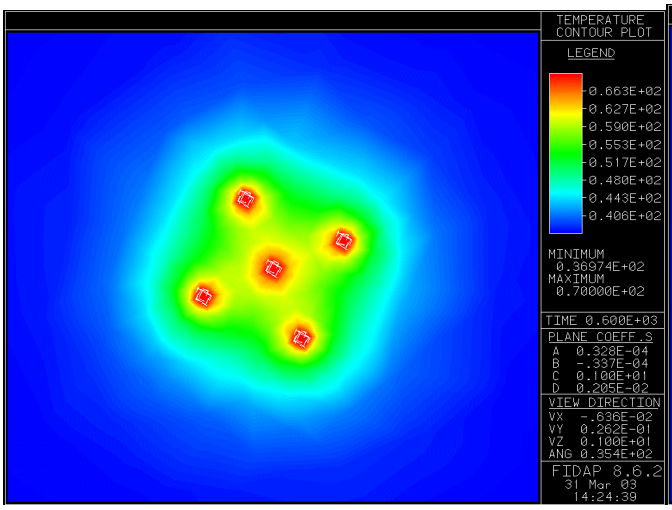

***Figure 3**: Magnified radial temperature contour plot of the probes at 70°C after 600 seconds of heating*

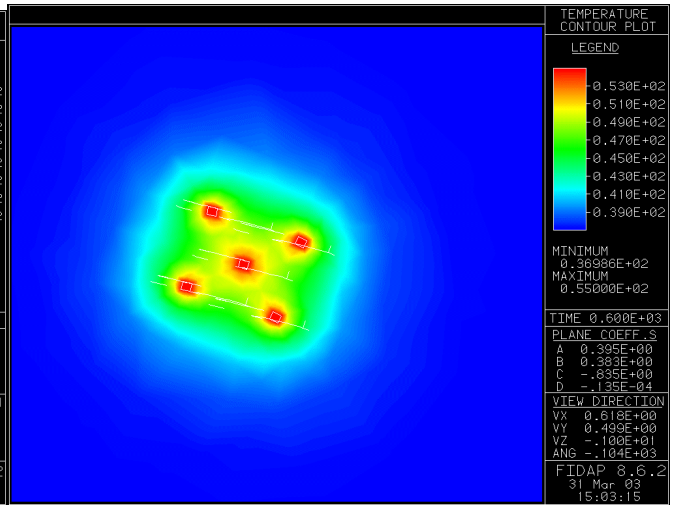

***Figure 4**: Magnified radial temperature contour plots of probes at 55°C after 600 seconds of heating*

Rod Placement Optimization

The five ferromagnetically heated probes create a "kill-zone" which radiates outward with time. A kill-zone is defined as the volume of tissue that experiences temperatures of 45°C or greater. 45°C is the minimum temperature required to successfully destroy cancerous tissue. The probes with radius 0.5mm and length 14mm must be positioned in such a way that the kill-zone encompasses the tumor, but not the healthy tissue. Optimizing probe geometry therefore depends on the shape of the tumor. In this project we will assume that the tumor is cylindrical. Consequently three-dimensional kill-zone should also be cylindrical. Three trials were run with different rod geometry. Each model placed one probe in the center with the other four equidistant probes surrounding it.

In trial one, the outer rods had a 5mm radius of separation from the center rod. The heating pattern created is shown below in Figures 5 and 6. This arrangement created a cylindrical "kill-zone" of 3.88cm^3, which would limit it to use on smaller tumors. To increase the size of the kill-zone, the probes must be separated.

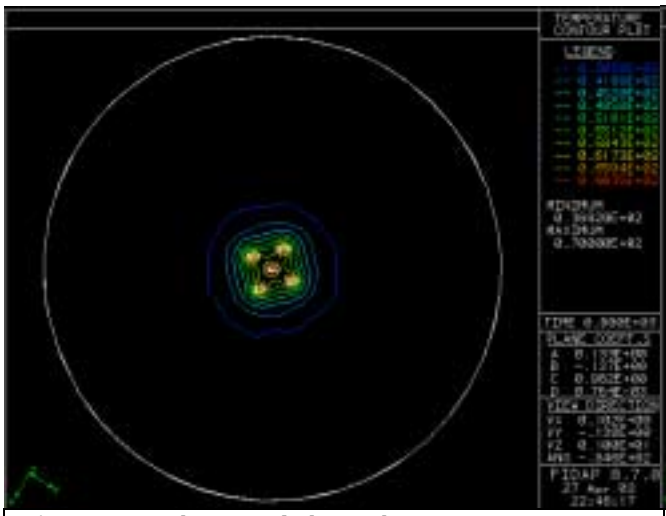

Figure 5: *Trial 1- A radial view line temperature contour plot for a five-probe separation of 5mm (Rods are at 70°C). The teal line is at 45°C and represents the boundary of the kill-zone.*

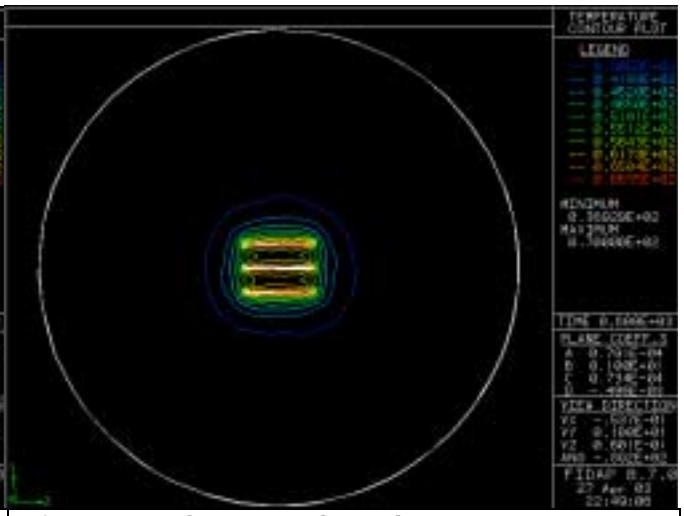

Figure 6: *Trial 1- An axial view line temperature contour plot for a five-probe separation of 5mm (Rods are at 70°C). The teal line is at 45°C and represents the boundary of the kill-zone.*

In trial two the probe separation was changed to 7.5mm. This created a semi-cylindrical kill-zone with a volume of 4.73cm^3 that is significantly bigger than the kill-zone produced in trial one. The temperature contour plots for trial two are displayed below in Figures 7 and 8. This arrangement creates a nearly cylindrical kill-zone, and also spans a large volume.

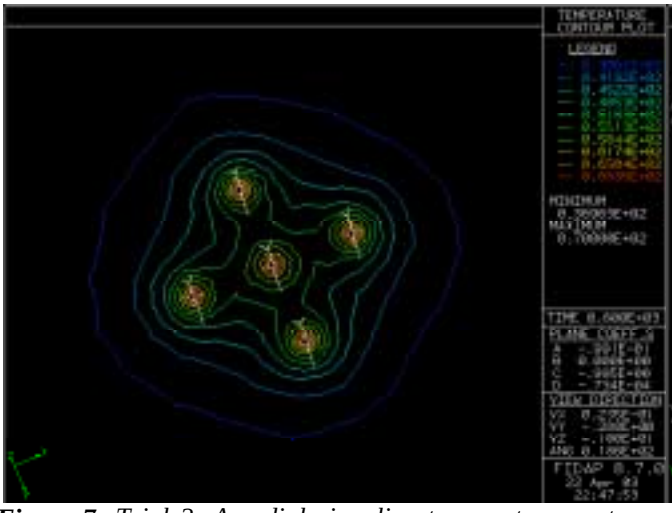

Figure 7: *Trial 2- A radial view line temperature contour plot for a five-probe separation of 7.5mm (Rods are at 70°C). The teal line is at 45°C and represents the boundary of the kill-zone.*

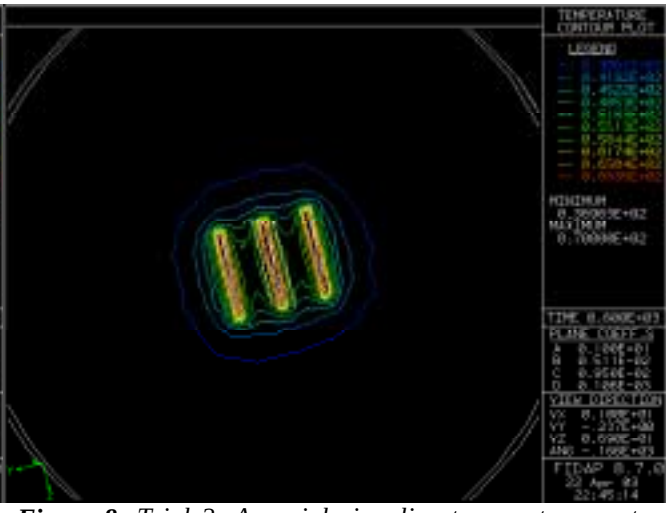

Figure 8: *Trial 2- An axial view line temperature contour plot for a five-probe separation of 7.5mm (Rods are at 70°C). The teal line is at 45°C and represents the boundary of the kill-zone.*

In the trial three, a 10mm separation radius was tested. The temperature contour plots displayed below in Figures 9 and 10 indicate that this setup is inefficient. The distance between the probes was too large,

causing a distortion in the kill-zone. Positioning the probes 10mm from the center of the model would not successfully eradicate a cylindrical tumor because of the uneven heating pattern.

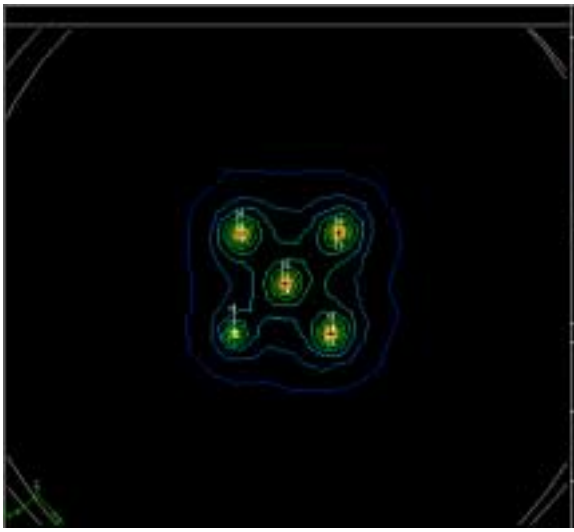

Figure 9: *Trial 3- A radial view line temperature contour plot for a five-probe separation of 10mm (Rods are at 70°C). The teal line is at 45°C and represents the boundary of the kill-zone.*

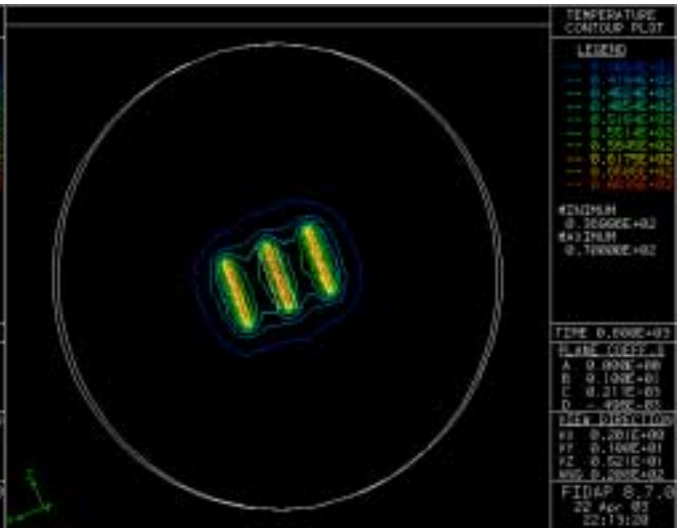

Figure 10: *Trial 3- An axial view line temperature contour plot for a five-probe separation of 10mm (Rods are at 70°C). The teal line is at 45°C and represents the boundary of the kill-zone.*

Parameter Sensitivity Analysis

To assess the sensitivity of our simulation to variations in key control variables, we measured the effects of changes in the •-term, which encompasses thermal conductivity, density, and specific heat, and the generation term, which is used to describe the blood flow perfusion effects. The two plots below show the relationship between the temperature found at node 1828, a reference node within the kill-zone, and the parameters (•, Q’’’).

The temperature varies linearly with the •-term. The •-term is the ratio of conductivity to the product of density and specific heat. As we increase the alpha term to 50%, 100%, 150% and 200% its original value, we are essentially increasing conductivity while decreasing density and specific heat. As conductivity increases, heat transfers more easily. Specific heat is the amount of heat per unit mass require to raise the temperature by one degree Celsius. As specific heat decreases, less heat is required to raise the temperature. Consequently an increase in alpha leads to an increase in temperature throughout the contour as indicated by Figure 11.

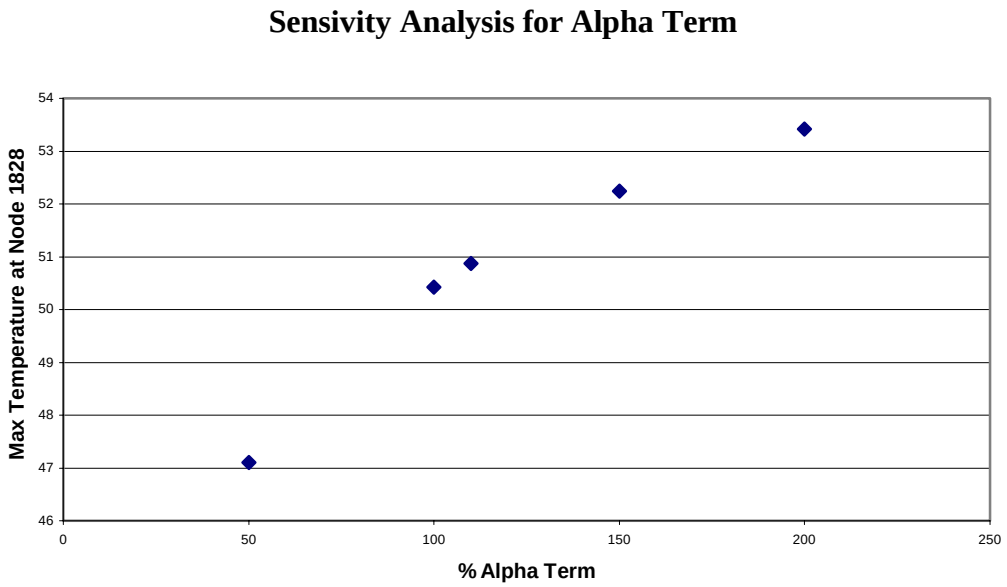

Figure 11: *The maximum temperature at node 1828 versus variation in the alpha term, which is the ratio of the thermal conductivity to the product of the density and specific heat.*

The temperature varies linearly with the blood perfusion term (Figure 12). This is a negative relationship because blood perfusion is a heat sink. The more blood perfusion cools the heated tissue, the lower the temperature will be throughout the contour.

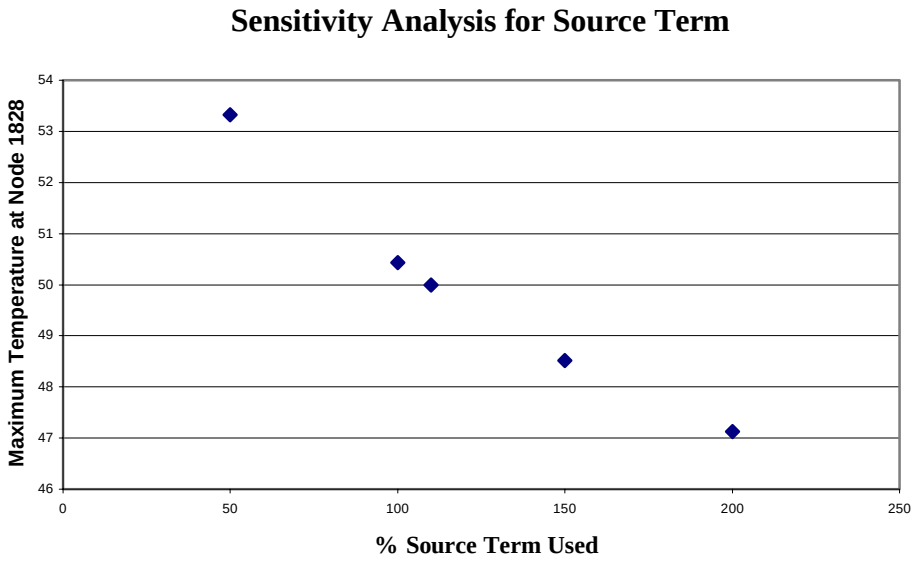

Figure 12: *The maximum temperature at node 1828 versus variation in the source (blood flow perfusion term) used. In the case of our model we used a "negative source" (i.e. a sink) to describe the behavior of the cooling effects of blood-flow perfusion.*

Conclusions and Design Recommendations

The ability of certain alloys to self regulate during inductive heating allows for phenomenal control over the ablation process. Depending on the size, location, and properties of a tumor, implanting an alloy with one Curie temperature may be more appropriate than another. Higher temperature rods will heat faster and with more intensity, which may be effective in treating tumors in the liver but not in the brain. Therefore the 70C heating probe can be used in less sensitive areas like hepatic tissue to produce fast and intense heating. The 55C probe can be used in more sensitive tissue like the brain to ablate slowly and safely.

In a preliminary model, only one probe was used (See Appendix C). This was determined to be ineffective because only a small volume could be treated. The ineffectiveness of one implant is consistent with results found in models of prostate heating performed by Tucker (2001). The model was expanded to five-rods, which allowed for adequate volumetric heating. The optimal placement of the five rods to maximize tumor ablation depends on the tumor shape. This is an inverse problem because we know that we want our kill-zone to be located at the boundary of the tumor, but the exact probe location that gives this result is unknown. Three different trials with different probe locations indicated that there is a tradeoff between the size of kill-zone and the kill-zone shape. For the five-probe geometry, spacing the rods close (5mm) allowed the kill-zone to be almost perfectly cylindrical. This would be ideal for treating a cylindrical tumor. The limitation is that the volume of the kill-zone is small and could therefore only treat small tumors. Spacing the rods radially 10mm from the center allowed the kill-zone to reach lager tumors, but its shape was distorted. This distortion would not optimally heat a large tumor and might lead to healthy tissue damage. Spacing the rods radially 7.5mm from the center proved to be the most efficient organization. The kill-zone was not significantly distorted from the optimal cylindrical shape and was large enough to destroy even big tumors. In clinical trials at the University of Chile and CharitÉ Hospital in Berlin rods were spaced no greater than 1cm to ensure uniform heating (Tucker 2000).

Although the development of ferromagnetic implants in cancer treatment is in the early stages, our five-rod model shows clearly that temperatures sufficient for ablation can be reached and controlled by the use of different alloy rods. Rod geometry can be adapted to destroy tumors of different sizes and shapes, provided that inter rod spacing is not beyond approximately 10mm. The main costs of this treatment are the alternating magnetic field device and the surgical implantation of the rods. Both these costs are comparable to the technology already in use in many hospitals. This treatment is feasible and will probably be implemented after more clinical trials are completed.

Appendix A: Mathematical Statement of Problem

The Biological Heat Transfer Equation is used to model temperature changes inside the liver due to ferromagnetic heating. The following key assumptions are made.

1) Metabolic heat generation is insignificant compared to the thermal processes.
2) Blood flow perfusion through liver is significant and is modeled as

$$Q''' = \rho c_{p-blood}\,\omega\left(T_{arterial} - T_{tissue}\right)$$

3) Large blood vessels are ignored and capillaries are isotropic.
4) Arterial blood temperature rapidly reaches tissue temperature.
5) The liver is homogeneous material with isotropic thermal properties.
6) The tumor and liver are modeled as solids and thus there is no internal convection.
7) Assume for the initial solution that heating of the ferromagnetic rod occurs rapidly enough to ignore the transient heating portion. There is actually transient heating, which will be accounted for later (Tucker 2001).
8) Assume for the initial solution that the properties of the tumor tissue and the hepatic tissue are constant and equal to each other.

The final energy equation is:

$$\rho C_{p-liver}\left(\frac{\partial T}{\partial t}\right) = k\left(\frac{\partial T}{\partial x} + \frac{\partial T}{\partial y} + \frac{\partial T}{\partial z}\right) + Q'''$$

Boundary Conditions

$$\mathrm{T}\Big|_{\text{implant edge}} = 343\ K$$

$$\mathrm{T}\Big|_{\text{infinite boundary}} = 310\ K$$

Initial Condition

$$\mathrm{T}\Big|_{t=0} = 310K$$

Properties (Tungjitkusolmun 2002)

$$\rho_{liver} = 1060\frac{kg}{m^3} \qquad \rho_{blood} = 1000\frac{kg}{m^3} \qquad k = .512\frac{W}{mK}$$

$$C_{p-liver} = 3600\frac{J}{kgK} \qquad C_{p-blood} = 4180\frac{J}{kgK} \qquad \omega = 6.4x10^{-3}\frac{1}{s}$$

Appendix B: FIDAP Input

PROBLEM Command
3-D (GEOMETRY TYPE): a portion of the liver was modeled as a sphere.
INCOMPRESSIBLE FLUID (FLOW REGIME): Blood flow was modeled using a heat sink and thus this project does not consider any fluid flow.
TRANSIENT (SIMULATION TYPE): The problem is not steady state as we are considering the change in temperature of the liver with respect to time.
LAMINAR (FLOW TYPE): Fluid flow is not considered in this project and thus this is not a factor.
LINEAR (CONVECTIVE TERM): Convection was not considered in this project.
NEWTONIAN (FLUID TYPE): A Newtonian fluid has a linear relationship between the applied shear stress and the rate of deformation.
NOMOMENTUM (MOMENTUM EQN): No fluid flow was considered in the project.
ENERGY (TEMPERATURE DEPENDENCE): Tells FIDAP to solve the energy equation for temperature.
FIXED (SURFACE TYPE): We made the assumption that all the surfaces remained unchanged.
NOSTRUCTURAL (STRUCTURAL SHAPE): The mesh is unstructured.
NOREMESHING (ELASTICITY REMESHING): We did not want the mesh t change throughout the process.
SINGLE PHASE (NUMBER OF PHASES): There were no phase changes.

SOLUTION Command
S.S. (Successive Substitution) = 10. The program does ten iterations of successive substititution within one time step.
ACCF = 0. Relaxation Factor, aids convergence by bringing the previous iteration into the current iteration. Zero is the constant value.

TIME INTEGRATION Command
Backward: The program uses the backward difference method for time integration.
NSTEPS = 2400. This allows the program to run 2400 discrete integration steps to find the solution.
TSTART = 0. This tells it to start the time at 0 seconds.
TEND = 600. This tells it to end the simulation at a time of 600 seconds.
DT = .25 The increment between steps is set at .25 seconds.

Mesh Convergence:

Mesh convergence was determined by examining the contour plots for two different meshes; an original mesh and a refined mesh. The original mesh was created using 2400 element and the refined mesh was created using 3200 elements. As you can see the contour plot for the original and refined mesh did not differ. Thus we can conclude that the original 2400 element mesh was adequately fine.

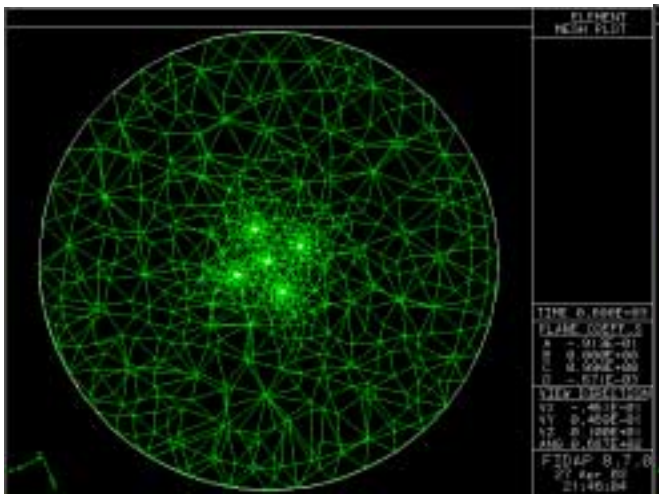

B1: *A radial view of the original five probe mesh*

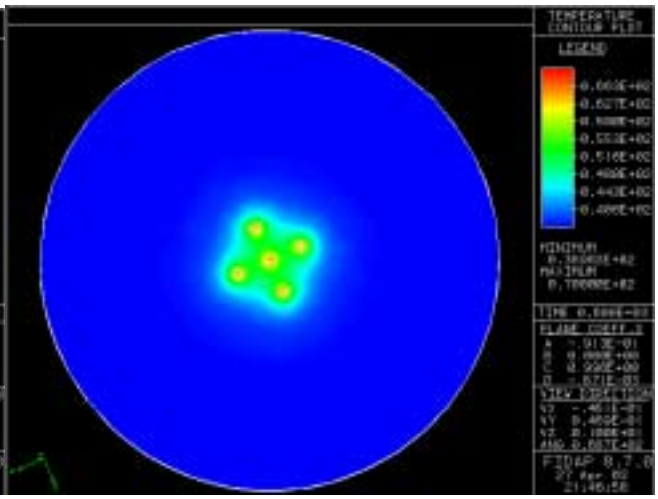

Figure B2: *A radial view of a the temperature contour plot obtained from the original mesh*

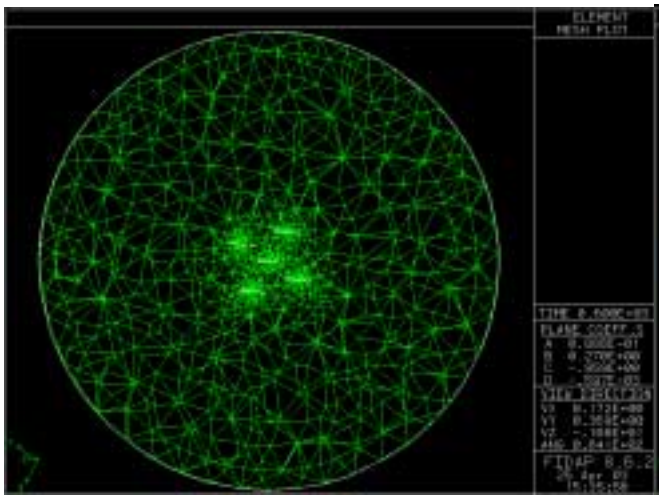

B3: *A radial view of the refined five probe mesh*

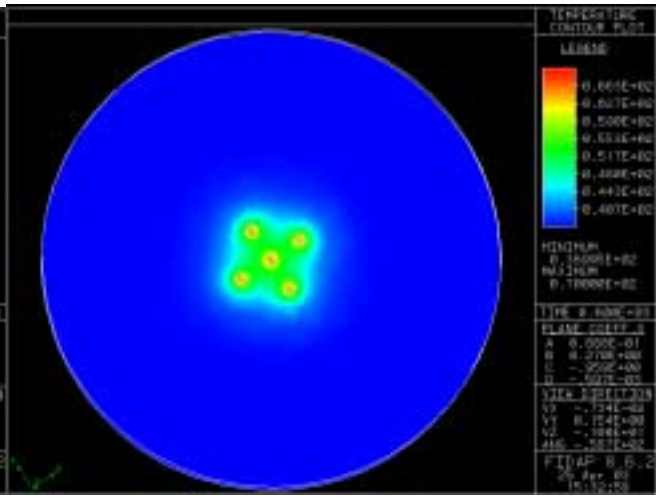

B4: *An radial view of a the temperature contour plot obtained from the original mesh*

Time Step Convergence:

One analysis to examine the accuracy of our model was a variation in the time step that FIDAP used to solved the simulation. In most of our analysis, we used a time step of 0.25 seconds. We reduced the time step to 0.1 seconds and repeated the analysis. Although 0.1 seconds more precise solutions, when compared to our original solution, there were no noticeable changes in the results. The lack of variation with respect to the time step strengthens the validity of our model. Below we present evidence for this with two different end contour plots. Both present the heating of the five implant spread at 600 seconds with a probe temperature (Curie Point) of 70 degrees Celsius. The only difference in the creation of the two plots is the latter was developed with a time step of 0.1 seconds. The plots clearly show no difference in the heat transfer.

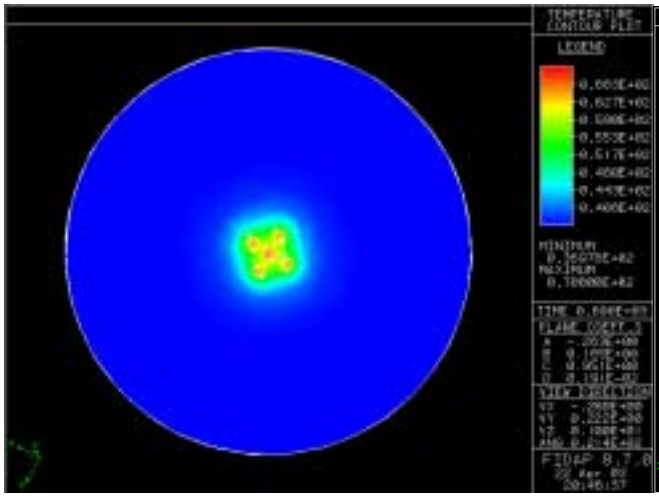

Figure B5: *Cross section of temperature plot with time step 0.25 seconds*

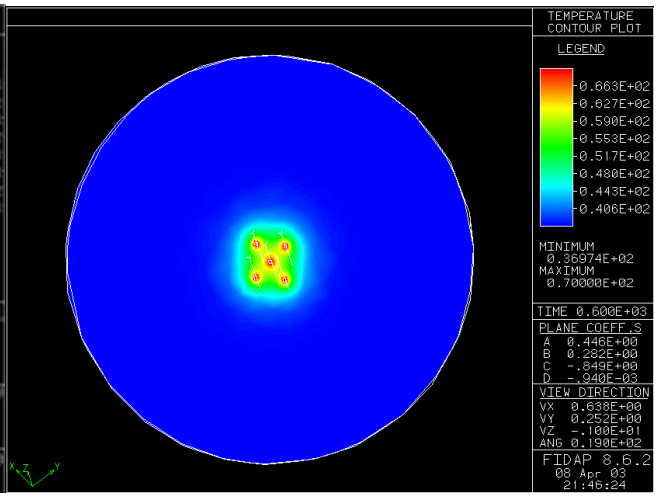

Figure B6: *Cross section of the temperature plot with time step 0.1 seconds.*

Appendix C: Additional Material and Background Derivations:

Axis-Symmetric Preliminary Solution with single rod implant

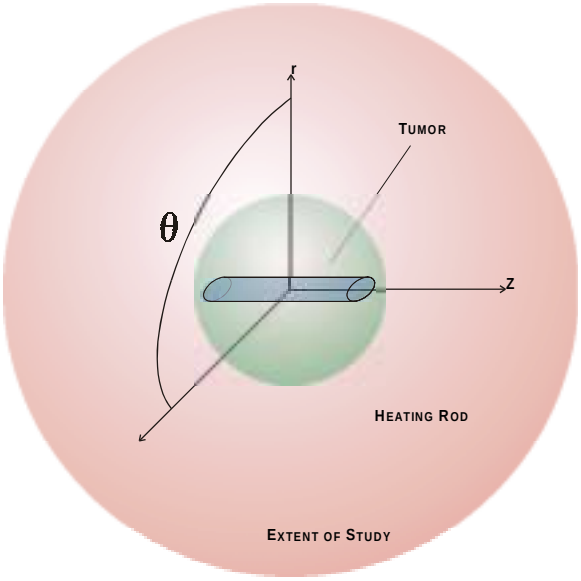

Figure C1: *Geometry used in computing the problem. The axial symmetries allow the three-dimensional topology displayed above to be reduced to a two-dimensional axis-symmetric simulation. NB: The "theta" angular dimension is present for reference, but is trivial in the simulation.*

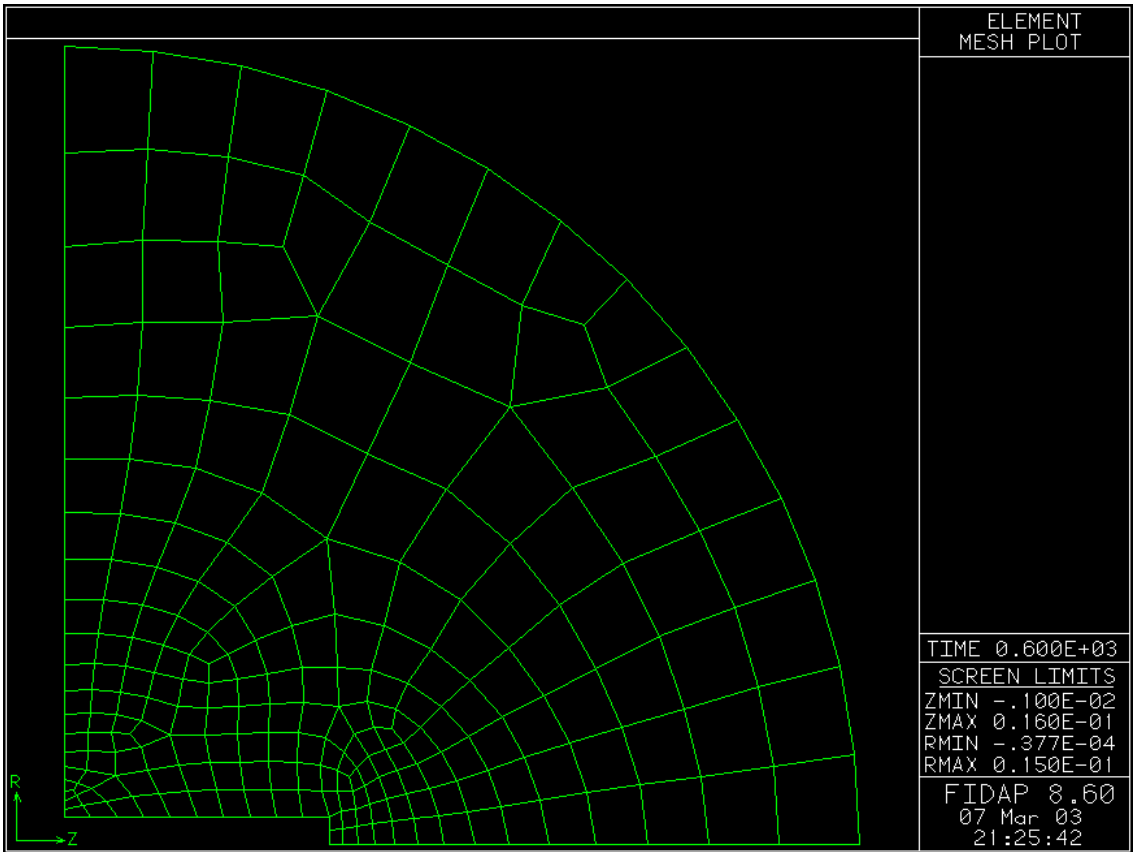

Figure C2: *Generated Mesh for Simulation Geometry- Nodes are concentrated near the probe where the effects of heating will be most concentrated.*

The Biological Heat Transfer Equation is used to model temperature changes inside the liver due to ferromagnetic heating. The following key assumptions are made.

1. Metabolic heat generation is insignificant compared to the thermal processes.
2. Blood flow perfusion through liver is significant and is modeled as:
$$Q''' = \rho C_{p-blood}\,\omega\left(T_{arterial} - T_{tissue}\right)$$
3. Large blood vessels are ignored and capillaries are isotropic.
4. Arterial blood temperature rapidly reaches tissue temperature.
5. The liver is homogeneous material with isotropic thermal properties.
6. The tumor and liver are modeled as solids and thus there is no internal convection.
7. Assume for the initial solution that heating of the ferromagnetic rod occurs rapidly enough to ignore the transient heating portion. There is actually transient heating, which will be accounted for later (Tucker 2001).
8. Assume for the initial solution that the properties of the tumor tissue and the hepatic tissue are constant and equal to each other.

The final energy equation is:

$$\rho C_{p-liver}\left(\frac{\partial T}{\partial t}\right) = k\left(\frac{1}{r}\frac{\partial}{\partial r}\left(r\frac{\partial T}{\partial r}\right) + \frac{\partial^2 T}{\partial z^2}\right) + Q$$

Boundary Conditions

$$-k\left.\frac{\partial T}{\partial r}\right|_{r=0} = 0 \quad \text{No flux at symmetric axis} \qquad \left.T\right|_{\text{implant edge}} = 343K$$

$$-k\left.\frac{\partial T}{\partial z}\right|_{z=0} = 0 \quad \text{No flux at symmetric middle} \qquad \left.T\right|_{\text{infinite boundary}} = 310k$$

Initial Condition

$$\left.T\right|_{t=0} = 310K$$

Properties (Tungjitkusolmun 2002)

$$\rho_{liver} = 1060\frac{kg}{m^3} \qquad \rho_{blood} = 1000\frac{kg}{m^3} \qquad k = .512\frac{W}{mK}$$

$$C_{p-liver} = 3600\frac{J}{kgK} \qquad C_{p-blood} = 4180\frac{J}{kgK} \qquad \omega = 6.4x10^{-3}\frac{1}{s}$$

Preliminary Solution

For our preliminary solution, we ignored the blood perfusion (Q’’’) term. As mentioned above, we assumed that the heating was instantaneous and that the tissue and liver properties were equal to each

other. We have included a temperature distribution from the simulation for an implantation time of 10 minutes.

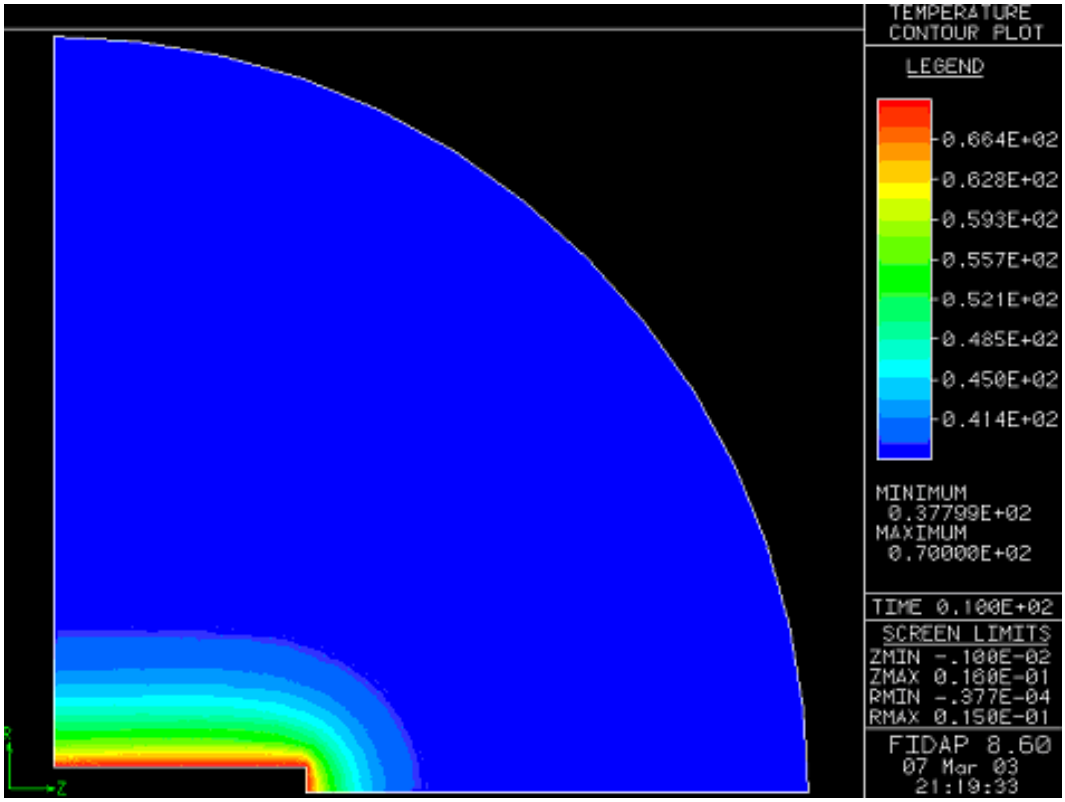

Figure C3: *Temperature Contour Plot after 10 seconds of heating*

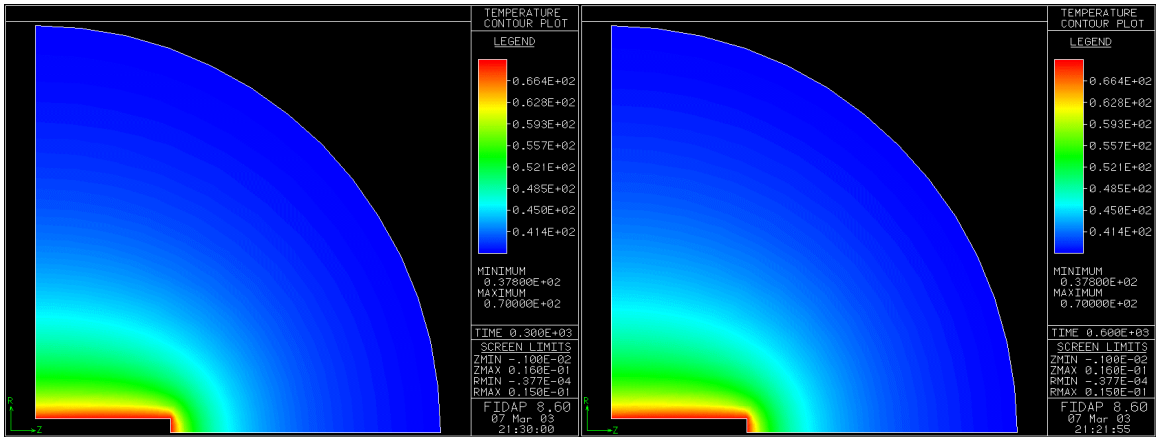

Figure C4: *(Left) Temperature Contour Plot after 300 seconds of heating and (right) Temperature Contour Plot after 600 seconds of heating.*

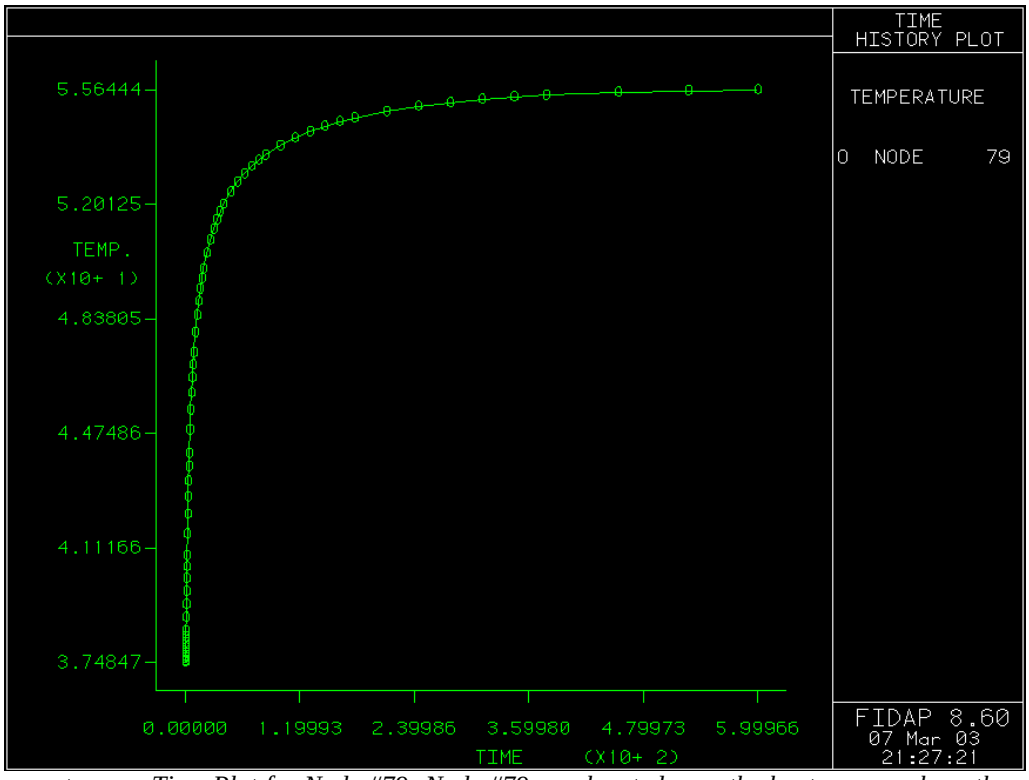

Figure C6: *Temperature vs. Time Plot for Node #79- Node #79 was located near the heat source where the effects of heating would be most dramatic.*

Analysis of Preliminary Solution for Constant Properties

As shown in Figure 4, when the heat source is stimulated for 10 minutes (600 seconds) tissue cells in a 5mm radius of the probe are destroyed. The light blue area of Figure 4 indicates the perimeter of the destroyed tissue. This area reaches a temperature of approximately 45°C, an efficient yet minimal temperature to destroy malignant tissue. Beyond this radius the tissue temperature is indicated by a darker blue color thus showing that the tissue is unaffected and unharmed by the heat source. Our simulation is therefore a semi-infinite model.

Appendix D: References

Paulus J.A., Parida G.R., Tucker R.D., Park J.B, Corrosion Analysis of NiCu and PdCo Thermal Seed Alloys Used As Interstitial Hyperthermia Implants, *Biomaterials* 18 (24), 1997.

Paulus J.A., Richardson J.S., Tucker R.D., Park J.B, Evaluation of Inductively Heated Ferromagnetic Alloy Implants for Therapeutic Interstitial Hyperthermia, *IEEE Transactions on Biomedical Engineering*, 43, (4) April 1996.

Tucker R.D., Huidobro C, Larson T, Platz C. The Use of Permanent Interstitial Temperature Self-Regulating Rods for Ablation of Prostate Cancer. *Journal of Endourology*, 14 (6), pp511-517, 2000.

Tucker, R.D. The Principle of Induction Heating for the Thermal Ablation of Tissue in Medical Applications. *Biomedical Engineering: University of Iowa College of Medicine*, http://www.ATImedical.com/clinical_publications.html, 2001.

Tungjitkusolmun S, Staelin ST, Haemmerich D, Tsai JZ, Webster JG, Lee FT Jr, Mahvi DM, Vorperian VR., Three-Dimensional Finite-Element Analyses for Radio-Frequency Hepatic Tumor Ablation, *IEE Transactions on Biomedical Engineering*, 49, pp 3-7, 2002.